Chemical Science

EDGE ARTICLE

View Article Online
View Journal | View Issue

Cite this: *Chem. Sci.*, 2017, **8**, 6257

A multi-signal fluorescent probe for simultaneously distinguishing and sequentially sensing cysteine/homocysteine, glutathione, and hydrogen sulfide in living cells†

Longwei He, Xueling Yang, Kaixin Xu, Xiuqi Kong and Weiying Lin*

Biothiols, which have a close network of generation and metabolic pathways among them, are essential reactive sulfur species (RSS) in the cells and play vital roles in human physiology. However, biothiols possess highly similar chemical structures and properties, resulting in it being an enormous challenge to simultaneously discriminate them from each other. Herein, we develop a unique fluorescent probe (**HMN**) for not only simultaneously distinguishing Cys/Hcy, GSH, and H_2S from each other, but also sequentially sensing Cys/Hcy/GSH and H_2S using a multi-channel fluorescence mode for the first time. When responding to the respective biothiols, the robust probe exhibits multiple sets of fluorescence signals at three distinct emission bands (blue-green-red). The new probe can also sense H_2S at different concentration levels with changes of fluorescence at the blue and red emission bands. In addition, the novel probe **HMN** is able to discriminate and sequentially sense biothiols in biological environments *via* three-color fluorescence imaging. We expect that the development of the robust probe **HMN** will provide a powerful strategy to design fluorescent probes for the discrimination and sequential detection of biothiols, and offer a promising tool for exploring the interrelated roles of biothiols in various physiological and pathological conditions.

Received 27th January 2017
Accepted 26th June 2017

DOI: 10.1039/c7sc00423k

rsc.li/chemical-science

Introduction

Biothiols are essential reactive sulfur species (RSS) in cells and they play vital roles in human physiology, such as the regulation of oxidative stress, signal transduction, and chelation of metal ions.[1–5] Hydrogen sulfide (H_2S), the simplest biothiol, has been considered as the gaseous signal molecule following nitric oxide (NO) and carbon monoxide (CO).[6] The physiological level of H_2S maintains the balance of intracellular redox status and regulates fundamental signaling processes including cardiovascular functional regulation, insulin secretion, neurotransmission, and apoptosis.[7–10] Cysteine (Cys) and homocysteine (Hcy) are two very similar biothiols, both of which are precursors of H_2S, which can be endogenously produced by enzymes such as cystathionine β-synthase (CBS) and cystathionine γ-lyase (CSE), displaying vital functions in the regulation of matrix degradation and cell motility.[11–13] Glutathione (GSH), the most abundant intracellular non-protein biothiol, is synthesized from its constituent amino acids by the consecutive actions of γ-glutamylcysteine synthetase (GSH I) and glutamine synthetase (GSH II).[14] GSH also plays important roles in combating oxidative stress and defending against free radicals to protect thiol proteins and enzymes from oxidation.[15] As shown in Fig. 1, the H_2S level is tightly associated with the Cys, Hcy, and GSH levels in living systems, and the level fluctuations of one biothiol may have a significant impact on others. Hence, it is of great significance to simultaneously distinguish and sequentially detect Cys/Hcy, GSH, and H_2S in bio-systems, and this is beneficial for gaining a better understanding of their generation and metabolic mechanisms and physiological functions in biological systems.

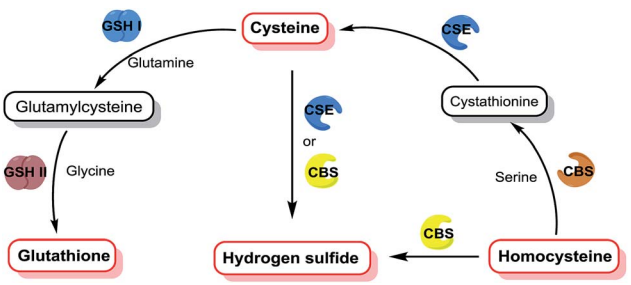

Fig. 1 The relationship between generation and metabolic pathways of different biothiols.

Institute of Fluorescent Probes for Biological Imaging, School of Chemistry and Chemical Engineering, School of Materials Science and Engineering, University of Jinan, Shandong 250022, P. R. China. E-mail: weiyinglin2013@163.com

† Electronic supplementary information (ESI) available: Experimental details for chemical synthesis of all compounds, chemical structure characterization, supplementary spectra of probe, and fluorescence imaging methods and data. See DOI: 10.1039/c7sc00423k

Recently, fluorescent probes have attracted a great deal of attention due to the advantages of high selectivity, high sensitivity, and real-time and non-destructive visual detection.[16–22] Therefore, it is interesting to engineer fluorescent probes for simultaneously distinguishing and sequentially detecting Cys/Hcy, GSH, and H_2S. Owing to the similar chemical structures and properties of these biothiols, it is very challenging to distinguish Cys/Hcy, GSH, and H_2S from each other. For instance, all of them have a nucleophilic sulfhydryl group (–SH) and the pK_a of H_2S (6.9) is lower than that of Cys (8.3), Hcy (8.9), or GSH (9.2), indicating that H_2S has a stronger nucleophilicity than other biothiols under physiological conditions. Hence, it is very difficult to distinguish Cys/Hcy/GSH from H_2S simply *via* nucleophilic reaction-based strategies. Pluth *et al.* found that the dark 4-chloro-7-nitro-1,2,3-benzoxadiazole (**NBD-Cl**) could perform a turn-on fluorescence in response to Cys *via* consecutive nucleophilic substitution and intramolecular rearrangement reactions, while the emission would be quenched again *via* another stronger nucleophilic substitution reaction by H_2S.[23] Three independent groups led by Guo, Goswami, and Zhao reported three merocyanine-based fluorescent probes for the ratiometric detection of H_2S without interference from other biothiols through the addition reaction of S^{2-}/HS^- with an indolium moiety.[24–26] To the best of our knowledge, although a number of fluorescent probes for selectively detecting Cys/Hcy, GSH, or H_2S have been designed (Table S1†),[27–34] there is no reported probe that can simultaneously distinguish Cys/Hcy, GSH, and H_2S from each other.

Herein, we subtly connected a hydroxyphenyl benzothiazole merocyanine (HBTMC) fluorophore and a nitro benzoxadiazole (NBD) chromophore using an ether linker as a new hybrid fluorescent dyad (**HMN**) (Scheme 1). The HBTMC moiety served as a recognition unit for the selective response to H_2S, and the functional NBD moiety was designed for the selective detection of Cys/Hcy and the sequential sensing of Cys/Hcy/GSH and H_2S. The **HMN** probe might be inherently non-fluorescent due to the protected hydroxyl NBD chromophore and quenching of the fluorescence of the HBTMC moiety by the NBD moiety. As shown in Scheme S1,† reaction of **HMN** with Cys/Hcy may cut off the ether bond, releasing the HBTMC unit and forming an amino substituted NBD chromophore (**NBD-Cys/Hcy**) after sequential nucleophilic substitution and intramolecular rearrangement, which will result in lighting up in green and red emission. Meanwhile, reaction of **HMN** with GSH may produce free **HBTMC1** and a dark mono-substituted sulfhydryl NBD (**NBD-GSH**) *via* a one step nucleophilic substitution reaction, giving off only red emission (Schemes 1 and S1†). If **HMN** reacts with the stronger nucleophilic reagent H_2S, the ether bond would also be cut off to yield a dark non-substituted sulfhydryl NBD chromophore (**NBD-SH**) and a free HBTMC chromophore (**HBTMC1**). In addition, the C=N double bond of **HBTMC1** would be further added by HS^- to afford an interrupted HBTMC derivative (**HBTMC-SH**), generating a new blue emission. Thus, **HMN** can discriminate Cys/Hcy, GSH, and H_2S with three different sets of fluorescence signals in three channels. In addition, if H_2S continues to be added to the mixture of **HMN** and Cys/Hcy, the intermediate product **NBD-Cys/Hcy** would be further substituted and **HBTMC1** would be attacked by the HS^- anion to yield dark **NBD-SH** and blue fluorescent **HBTMC-SH**, accompanied by quenching of both green and red emission (Schemes 1 and S1†). Similarly, the intermediate product **HBTMC1** from the reaction of **HMN** with GSH could also react with H_2S, and synchronously light up fluorescence in the blue emission channel (Schemes 1 and S1†). Taken together, the dyad **HMN** is capable of not only simultaneously distinguishing Cys/Hcy, GSH, and H_2S from each other but also sequentially detecting Cys/Hcy (or GSH) and H_2S through the changes of three well-defined emission bands (blue-green-red).

Results and discussion

Design and synthesis of probes

Due to the strong electron withdrawing ability of the 7-position nitro group, the functional group at the 4-position is easily substituted by nucleophilic reagents, such as sulfhydryl-containing biothiols, in the NBD chromophore. Many NBD derivatives have been employed for the selective detection of Cys/Hcy or the sequential detection of biothiols.[32,33,36–38] In addition, the group of carbon–nitrogen double bonds in electropositive merocyanine and cyanine dyes can be interrupted by

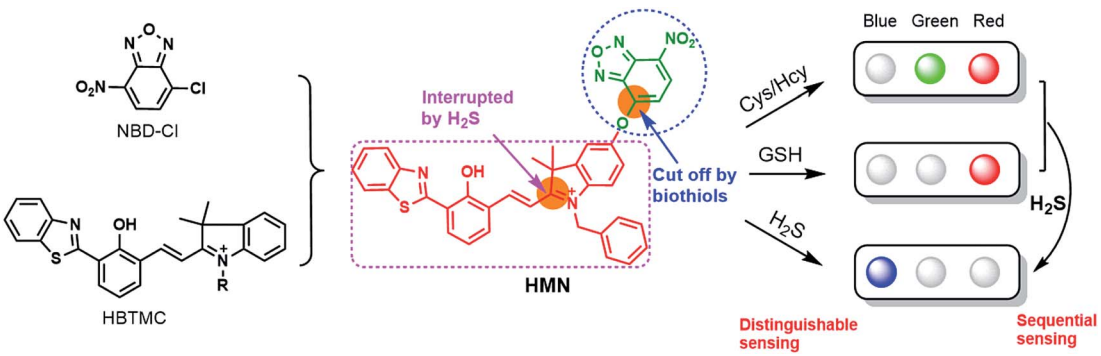

Scheme 1 The design strategy of the probe **HMN** and the proposed fluorescence signal changes in response to respective biothiols or sequential biothiols with three well-defined emission bands.

strongly nucleophilic reagents (such as S^{2-} and HS^- anions), while it is barely attacked by the relatively moderate nucleophile like mono-substituted sulfhydryl reagents (RSH).[24–26,39] Accordingly, merocyanine dyes are the preferred platforms for designing fluorescent probes for distinguishing H_2S from other biothiols. Thus, we rationally designed a hybrid fluorophore (**HMN**) of hydroxyphenyl benzothiazole merocyanine (HBTMC) and nitro benzoxadiazole (NBD) through an ether group for simultaneously distinguishing and sequentially sensing Cys/Hcy/GSH and H_2S. The synthetic route of probe **HMN** is outlined in Scheme S2,† and intermediate products **1**, **3**, and **HBTQ** were prepared according to previous methods.[40–42] The target product was synthesized through a nucleophilic substitution reaction of dihydroxyl **HBTMC1** and **NBD-Cl** with desirable yield, and the results of the control experiment indicate that monohydroxyl **HBTMC2** can barely react with **NBD-Cl**, due to the considerable steric hindrance. All new compounds were well characterized using mass spectrometry and NMR spectroscopy (for synthesis and characterization details, see the ESI†).

Spectral response of the probe to biothiols

With probe **HMN** in hand, we firstly investigated the spectra of **HMN** (10 μM) in order to separate biothiols in phosphate buffer solution (25 mM, pH 7.4, containing 20% acetonitrile). In spectrofluorometric titrations, free **HMN** has no fluorescence in the visible region. Upon addition of increasing dosages of Cys or Hcy (from 0 to 1.0 mM), the mixture exhibits two new green and red emission bands centered at 546 nm (excited at 470 nm) and 609 nm (excited at 550 nm), respectively (Fig. 2A and B). This may be attributed to the products **HBTMC1** and amino NBD (**NBD-Cys**/**NBD-Hcy**) from the sequential nucleophilic substitution and intramolecular rearrangement reactions of **HMN** with Cys/Hcy. When GSH (from 0 to 1.0 mM) was added to the probe solution, only a gradual increase of the red emission was observed (Fig. 2C), indicating that the reaction of the probe with GSH generates red fluorescent **HBTMC1** and dark mono-substituted sulfhydryl NBD (**NBD-GSH**). When probe **HMN** encounters increasing amounts of H_2S (from 0 to 5.0 mM), the mixture responds with the emergence of red emission, like GSH as the H_2S concentration ranged from 0–0.5 mM (Fig. 2D). However, as the H_2S concentration continues to increase, the emerging red emission begins to weaken and synchronously generates a new blue emission band centered at 485 nm (excited at 410 nm). These results can be interpreted to mean that probe **HMN** is cut off by H_2S at a low concentration (abbreviated as H_2S(LC)) and produces the red fluorescent chromophore **HBTMC1** and non-fluorescent non-substituted sulfhydryl NBD (**NBD-SH**), while the intermediate product **HBTMC1** is further attracted by H_2S at a high concentration (abbreviated as H_2S(HC)) and yields the blue fluorescent compound **HBTMC1-SH**. As the intensity of the newly generated emission reaches the maximum values, Cys/Hcy induces a 53.4/57.6 and 32.2/32.9-fold enhancement of the fluorescence intensity at 546/609 nm, GSH induces 33.6-fold enhancement of intensity at 609 nm, and H_2S(LC)/H_2S(HC) generates a 17.7/52.7-fold increase of intensity at 609/485 nm (Fig. 3). Accordingly, the fluorescent colour of **HMN** was changed from dim to orange, pink, and blue by the addition of Cys/Hcy, GSH/H_2S(LC), and H_2S(HC), respectively (Fig. S1†). Furthermore, all biothiols have good linear relationships with the maximum intensity values of newly generated red emission bands in a certain concentration range (Fig. S2†), and accordingly the limit of detection (defined by $3\sigma/k$, where σ is the standard deviation of the blank sample and k is the slope of the linear regression equation) is calculated to be 4.25, 5.11, 4.30, and 6.74 μM for Cys, Hcy, GSH, and H_2S, respectively. In the reaction-time study, when the changes of fluorescence intensity are completed, the intensity values at 546 and 609 nm reach plateaus 12/20 and 15/20 min after adding 55 equivalents of Cys/Hcy, respectively (Fig. S2b and c†). The new red emission induced by GSH (65 equiv.) or H_2S(LC) (50 equiv.)

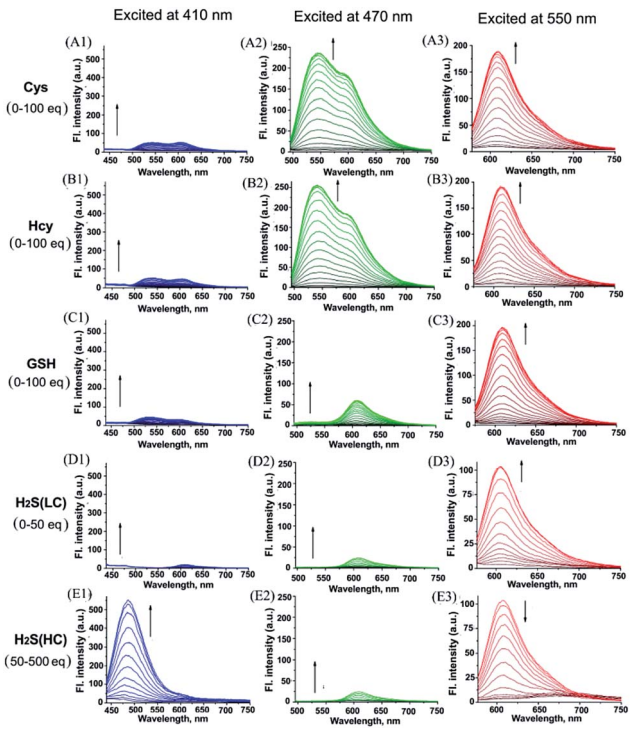

Fig. 2 The titration fluorescence spectra of **HMN** (10 μM) upon addition of (A) Cys (0–100 equiv.), (B) Hcy (0–100 equiv.), (C) GSH (0–100 equiv.), (D) H_2S(LC) (0–50 equiv.), and (E) H_2S(LC) (50–500 equiv.) in PBS (25 mM, pH 7.4, containing 20% acetonitrile). Excitation at 410 nm for the first column, 470 nm for the second column, and 550 nm for the third column. H_2S(LC) and H_2S(HC) denote H_2S at low and high concentration, respectively.

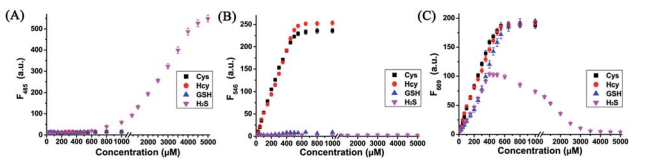

Fig. 3 The fluorescence intensity of **HMN** (10 μM) at (A) 485 nm, (B) 546 nm, and (C) 609 nm upon addition of Cys (0–100 equiv.), Hcy (0–100 equiv.), GSH (0–100 equiv.), and H_2S (0–500 equiv.) in PBS (25 mM, pH 7.4, containing 20% acetonitrile), respectively. Excitation at 410 nm for (A), 470 nm for (B), and 550 nm for (C).

reaches the steady state within 20 and 4 min, respectively, and the value of intensity at 485 nm induced by H_2S(HC) (500 equiv.) reaches a maximum within about 2 min (Fig. S3a and c†). Therefore, probe **HMN** is capable of simultaneously distinguishing Cys/Hcy, GSH, and H_2S from each other and sensing H_2S at different concentration levels through the changes of three well-defined emission bands (blue-green-red), which possess 61 and 63 nm interval distances between two adjacent bands respectively.

To shed light on the response process, the absorption spectra of **HMN** were also investigated in aqueous solution. As shown as in Fig. S4a,† free **HMN** exhibits two characteristic absorption peaks of NBD and HBTMC at 373 and 577 nm, respectively. Upon addition of Cys/Hcy, the absorption peak of HMTMC slightly blue shifts to 563 nm and a shoulder peak simultaneously emerges at about 485 nm, which can be attributed to the products **HBTMC1** and **NBD-Cys/Hcy** from reaction of **HMN** with Cys/Hcy. Similarly, the absorption peaks of **HBTMC1** and **NBD-GSH** are observed at 563 and 435 nm in the presence of GSH. When adding increasing dosages of H_2S, both of the two peaks of **HMN** gradually fade, and this is accompanied by the emergence of a broad peak at about 554 nm, which should contain two absorption peaks of **HBTMC1** and **NBD-SH**. To confirm the original attribution of those newly generated absorption peaks, the absorption spectra of control compounds **NBD-Cl** and **HBTMC1** in the presence of the respective biothiols were studied, and the results are coincident with the spectral performance of **HMN** (Fig. S4b and c†). Furthermore, the mass spectra of **HMN** in the respective biothiols were also measured in order to confirm the proposed reaction processes. As shown in Fig. S5,† the peaks of the key products **HMBMC1** (m/z = 503.2) and **NBD-Cys** (m/z = 284.3) are observed in the mixture of **HMN** and **Cys**. In a similar way, the peaks of **NBD-Hcy** (m/z = 299.2), **NBD-GSH** (m/z = 471.1), and **NBD-SH** (m/z = 197.1) appear in the spectra of **HMN** in the presence of Hcy, GSH, and H_2S respectively, while treatment with a high concentration of H_2S generates compound **HBTMC1-SH** (m/z = 536.2) (Fig. S6–9†). Therefore, the results of the measured absorption spectra and mass spectra of **HMN** in the presence of various biothiols agree with the proposed reaction mechanism.

Furthermore, we also investigated the spectral response of **HMN** upon successive addition of Cys/Hcy/GSH, and H_2S in aqueous solution. Upon continuing addition of greatly excessive amounts of H_2S to the mixture of **HMN** and Cys, both green and red emission gradually fade away and, synchronously, significant emission in the blue channel is generated (Fig. 4A). A similar phenomenon occurs in the mixture of **HMN** and Hcy (Fig. 4B). This could be ascribed to the idea that products **HBTMC1** and **NBD-Cys/Hcy** from the reaction of the probe with Cys/Hcy further react with the subsequent H_2S, yielding an interrupted merocyanine dye **HBTMC1-SH** and non-fluorescent **NBD-SH**. When adding excessive H_2S to the **HMN** and GSH mixture, the increasing blue emission accompanied by gradually weakening red emission is also observed (Fig. 4C). Accordingly, the orange (or pink) fluorescence of **HMN** induced by Cys/Hcy (or GSH) was finally changed to bright blue emission by the subsequent addition of H_2S (Fig. S10†). In the absorption

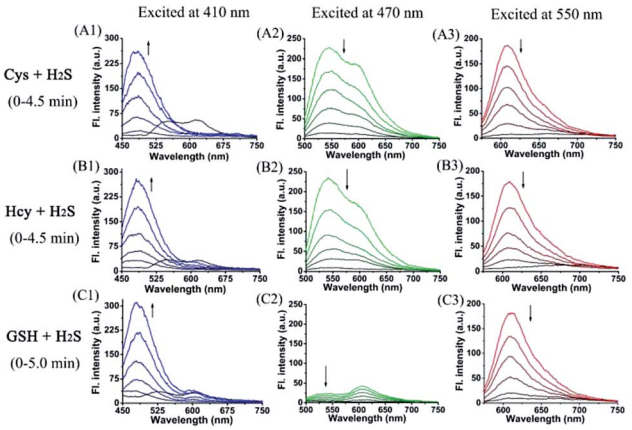

Fig. 4 The fluorescence spectra of **HMN** (10 μM) pre-treated with (A) Cys (100 equiv.), (B) Hcy (100 equiv.), and (C) GSH (100 equiv.) upon continued addition of H_2S (500 equiv.) within 4.5 (or 5.0) min in PBS (25 mM, pH 7.4, containing 20% acetonitrile). Excitation at 410 nm for the first column, 470 nm for the second column, and 550 nm for the third column.

spectra, the weakness of the **HBTMC1** absorption and disappearance of the **NBD-Cys/Hcy** absorption proves that **HMN** can react with Cys/Hcy/GSH and H_2S sequentially (Fig. S11†). The results indicated that probe **HMN** not only can simultaneously distinguish Cys/Hcy, GSH, and H_2S from each other, but also can sequentially sense Cys/Hcy/GSH and H_2S with three-channel fluorescence signal changes.

To evaluate the selectivity of probe **HMN** for biothiols, the specificity of **HMN** was tested in the presence of various relevant biological amino acids, anions, cations, ROS, and RNS, including alanine (Ala), arginine (Arg), aspartic acid (Asp), glutamic acid (Glu), isoleucine (Ile), phenylalanine (Phe), serine (Ser), threonine (Thr), tryptophan (Trp), valine (Val), histidine (His), VC, AcO^-, Br^-, Cl^-, NO_3^-, NO_2^-, N_3^-, SO_3^{2-}, $S_2O_3^{2-}$, Cu^+, Ca^{2+}, Fe^{2+}, Fe^{3+}, Zn^{2+}, HClO, O_2^-, H_2O_2, TBHP, and NO. As shown in Fig. 5A, **HMN** exhibits negligible fluctuation of fluorescence intensity in all three emission bands upon treatment with 1 mM of these interfering species. However, remarkable enhancement of the fluorescence intensity at both 546 and 609 nm is observed after treatment with 550 μM Cys or Hcy; addition of GSH (650 μM) only produces a significant increase of intensity at 609 nm, while treatment of H_2S(LC) (500 μM) or H_2S(HC) (5000 μM) generates an obvious enhancement of intensity at 609 or 485 nm, respectively. This suggests that probe **HMN** can selectively detect Cys/Hcy, GSH, and H_2S without interference from relevant amino acids, ROS, and RNS through changes of three well-defined emission bands. In addition, the effect of environmental pH on the response of **HMN** was also studied. As shown in Fig. 5B, the fluorescence intensity of free **HMN** at all three emission bands is nearly not fluctuant in aqueous solutions with different pH values. However, at pH ranging from 7.0 to 8.0, probe **HMN** generates significant enhancement of the fluorescence intensity in both blue and red emission bands in the presence of Cys/Hcy; addition of GSH induces fluorescence enhancement in only

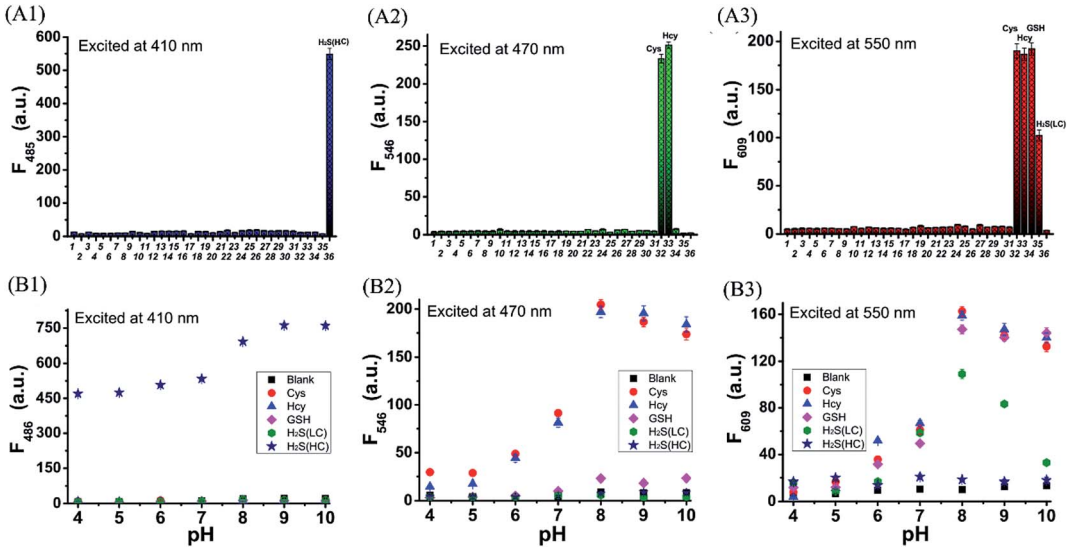

Fig. 5 (A) The fluorescence intensity of **HMN** (10 μM) at (A1) 485 nm, (A2) 546 nm, and (A3) 609 nm in the presence of (1) no interfering species, (2) Ala, (3) Arg, (4) Asp, (5) Glu, (6) Ile, (7) Phe, (8) Ser, (9) Thr, (10) Trp, (11) Val, (12) His, (13) VC, (14) AcO^-, (15) Br^-, (16) Cl^-, (17) NO_3^-, (18) NO_2^-, (19) N_3^-, (20) SO_3^{2-}, (21) $S_2O_3^{2-}$, (22) Cu^+, (23) Ca^{2+}, (24) Fe^{2+}, (25) Fe^{3+}, (26) Zn^{2+}, (27) HClO, (28) O_2^-, (29) H_2O_2, (30) TBHP, (31) NO, (32) Cys, (33) Hcy, (34) GSH, (35) H_2S(LC), and (36) H_2S(HC) in PBS (25 mM, pH 7.4, containing 20% acetonitrile). Concentrations were 1 mM for (2)–(30), 0.55 mM for (32) and (33), 0.65 mM for (34), 0.5 mM for (35), and 5.0 mM for (36). (B) The fluorescence intensity of **HMN** (10 μM) at (B1) 485 nm, (B2) 546 nm, and (B3) 609 nm in the presence or absence of biothiols at different pH values ranging 4.0–10.0 in PBS (25 mM, containing 20% acetonitrile). Concentrations were 0.55 mM for Cys/Hcy, 0.65 mM for GSH, 0.5 mM for H_2S(LC), and 5.0 mM H_2S(HC). Excitation at 410 nm for (A1/B1), 470 nm for (A2/B2), and 550 nm for (A3/B3). H_2S(LC) and H_2S(HC) denote H_2S at low and high concentrations, respectively.

the red emission band, and an increase of red or blue fluorescence is observed in the presence of H_2S(LC) or H_2S(HC), respectively. Thus, **HMN** has the potential to discriminatively detect biothiols under physiological conditions.

Theoretical study on the fluorescence mechanism

To better understand the spectral changes of probe **HMN** responding to biothiols, theoretical calculations were performed using density functional theory (DFT) with the B3LYP(d) exchange functional employing 6-31G* basis sets using a suite of Gaussian 09 programs. In the optimized structures of **HMN**, the dihedral angle of the HBT unit and indole unit is 92.6° in the conjugated HBTMC moiety, and the NBD moiety is also nearly perpendicular to indole group (86.3° angle), which suggests that the NBD moiety has a minimal impact on the electron delocalization degree of the HBTMC moiety (Fig. 6A).

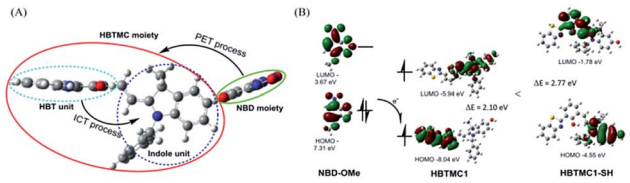

Fig. 6 (A) Optimized structures of **HMN** and the co-regulation of response emission by PET and ICT mechanisms. (B) Frontier molecular orbital energy of **NBD-OMe**, **HBTMC1**, and **HBTMC1-SH** at the excited state. Calculations were performed using DFT with the B3LYP exchange functional employing 6-31G* basis sets using Gaussian 09 programs.

Consequently, the emission of the HBTMC moiety should be regulated by the NBD unit *via* the photoinduced electron transfer (PET) process. To validate the proposed fluorescence mechanism, the frontier orbital energy of both separate NBD and HBTMC fluorophores was also calculated. As shown in Fig. 6B, the energy magnitude of the highest occupied molecular orbital (HOMO) of the oxyalkyl NBD chromophore (methoxyl NBD derivative, **NBD-OMe**) is between that of the lowest unoccupied molecular orbital (LUMO) and HOMO of the HBTMC chromophore (**HBTMC1**), indicating that the electron tends to transfer from the HOMO of NBD to the transition HOMO of HBTMC at the excited state. What's more, the π electrons on both the HOMO and LUMO efficiently distribute in the respective HBT and indole units in **HBTMC1**, suggesting that HBTMC is a typical intramolecular charge transfer (ICT)-based fluorophore. However, the product **HBTMC1-SH** from the addition reaction between **HBTMC1** and H_2S possesses a bigger energy difference between the LUMO and HOMO (2.77 eV) than that of **HBTMC1** (2.10 eV) (Fig. 6B), which can be ascribed to the interruption of the ICT process from the electron-donating HBT group to the electron-withdrawing indole group. Thus, the response emission of **HMN** to biothiols is regulated by the PET and ICT mechanisms together.

Discriminative detection of biothiols in living cells

Encouraged by the desirable spectral response of the probe to biothiols in aqueous solution, we then investigated the capability of **HMN** to detect biothiols in biological systems in a three-color manner (blue-green-red) using confocal fluorescence

microscopy. Before that, the cell cytotoxicity of **HMN** was evaluated using standard MTT assays, and these demonstrate that **HMN** has low cytotoxicity to living HeLa cells (Fig. S12†). For probe **HMN**, thiol- and amino-containing species are the most likely potential interferents for the imaging of biothiols in living systems. The selectivity assay suggested that treatment with amino-containing species (such as various amino acids) induced a very small amount of interference in the detection of biothiols (Fig. 5). In addition, we selected bovine serum albumin (BSA) as a model thiol-containing protein, and the spectral response of **HMN** to BSA was investigated. The results showed that negligible fluorescence fluctuation of the probe in the blue/green emission band and a small fluorescence fluctuation in the red emission band was generated in the presence of BSA (0–1000 μg mL^{-1}) in PBS (Fig. S13†). This might be because most of the sulfhydryls in BSA are present in the oxidized form (S–S), but both the reduced form (–SH) and the disulfide bonds exist stably in the physiological environment.[43,44] Thus, thiol-containing proteins have little effect on the detection of biothiols in living cells. In the control experiment, after being pre-treated with *N*-ethylmaleimide (NEM, a thiol scavenger, 0.5 mM), HeLa cells loaded with **HMN** (5 μM) exhibit very dim fluorescence in all three channels (Fig. 7A), which is in agreement with the emission spectral performance of the free probe in an aqueous system. For the experimental groups, the cells continued to be incubated with respective exogenous biothiols (Cys/Hcy/H_2S) after being pre-treated with NEM for 30 min. Upon continued treatment with Cys/Hcy (250 μM), significant enhancement of fluorescence in both the green (about 10.8/9.3-fold) and red (about 29.9/34.4-fold) channels is observed in the cells loaded with **HMN** (Fig. 7B and C). However, the cells treated with free **HMN** (5 μM) show a bright emission in the red channel (Fig. 7D), which indicates that **HMN** reacts with the most abundant cellular biothiol, GSH, and yields the strongly fluorescent **HBTMC1** chromophore. The cells pre-incubated with successive NEM and Na_2S (a donor for H_2S,[45] 2 mM) generate a remarkable increase in blue fluorescence (about 5.7-fold), while almost no fluorescence emission is observed in the green and red channels (Fig. 7E). Thus, **HMN** can discriminate cellular Cys/Hcy, GSH, and H_2S (at relatively high concentration levels) with three different sets of fluorescence signals *via* three-color fluorescence imaging.

In addition, we also carried out fluorescence imaging of exogenous H_2S and endogenous H_2S induced by Cys at a relatively low level in cells. As shown in Fig. S14,† after pre-treatment with NEM, the cells incubated with Na_2S (200 μM) show a slight and remarkable enhancement of fluorescence in the blue and red channels, respectively. However, upon pre-incubation with Cys (a precursor of H_2S,[46] 200 μM) for 1 hour, a similar fluorescence performance is observed to that resulting from the addition of a small dosage of Na_2S in living cells (Fig. S14c†), and this can be attributed to the endogenous production of H_2S stimulated by Cys. In brief, **HMN** can generate three or two distinct sets of fluorescence signals different from the control experiment in response to cellular biothiols (Cys/Hcy, GSH, and H_2S (at relatively high or low

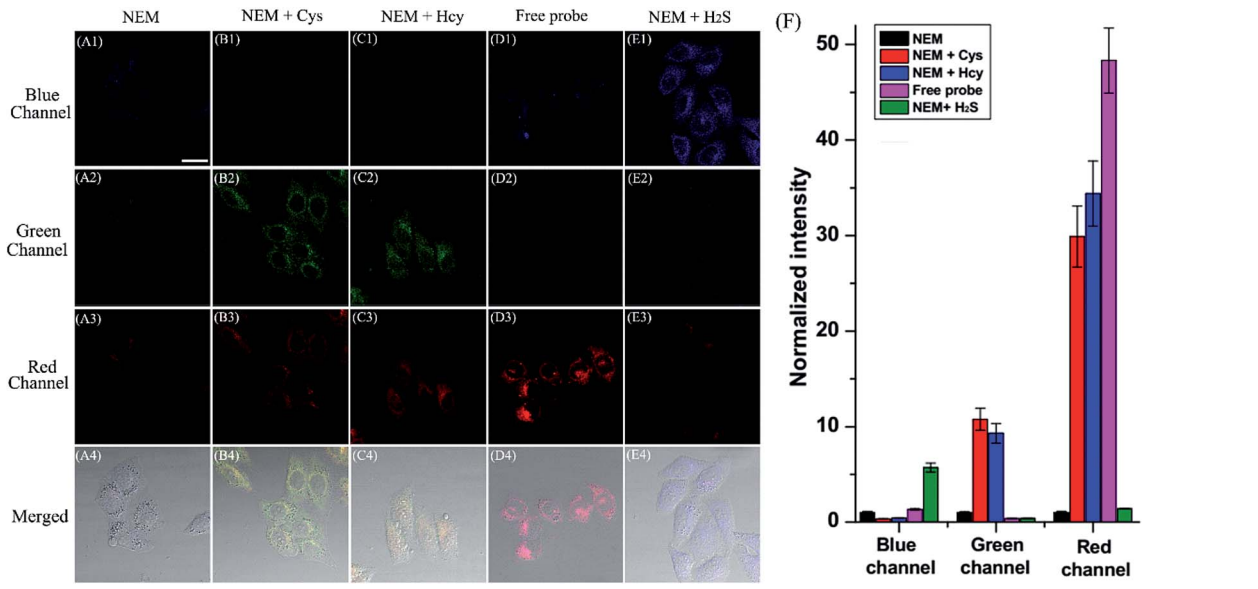

Fig. 7 Fluorescence images of probe **HMN** responding to respective biothiols in living HeLa cells using confocal fluorescence imaging. (A) Cells were pre-treated with NEM (0.5 mM, 30 min), subsequently incubated with probe **HMN** (5 μM, 30 min), and then imaged; (B and C) cells were pre-treated with NEM (0.5 mM, 30 min), subsequently incubated with Cys/Hcy (250 μM, 15 min) and probe **HMN** (5 μM, 30 min), and then imaged; (D) cells were incubated with probe **HMN** (5 μM, 30 min), and then imaged; (E) cells were pre-treated with NEM (0.5 mM, 30 min), subsequently incubated with Na_2S (2 mM, 15 min) and probe **HMN** (5 μM, 30 min), and then imaged. The fluorescence images were captured from the blue channel of 465–500 nm (first row), green channel of 525–555 nm (second row), and red channel of 595–630 nm (third row) with excitation at 405, 488, and 561 nm, respectively. Fourth row: merged bright field images with blue, green, and red channel images. Scale bar: 20 μm. (F) Normalized average fluorescence intensity of the blue, green, and red channels in (A–E). The normalized intensity of group (A) in the respective channels is taken as the reference standard. Data are expressed as the mean ± SD of three parallel experiments.

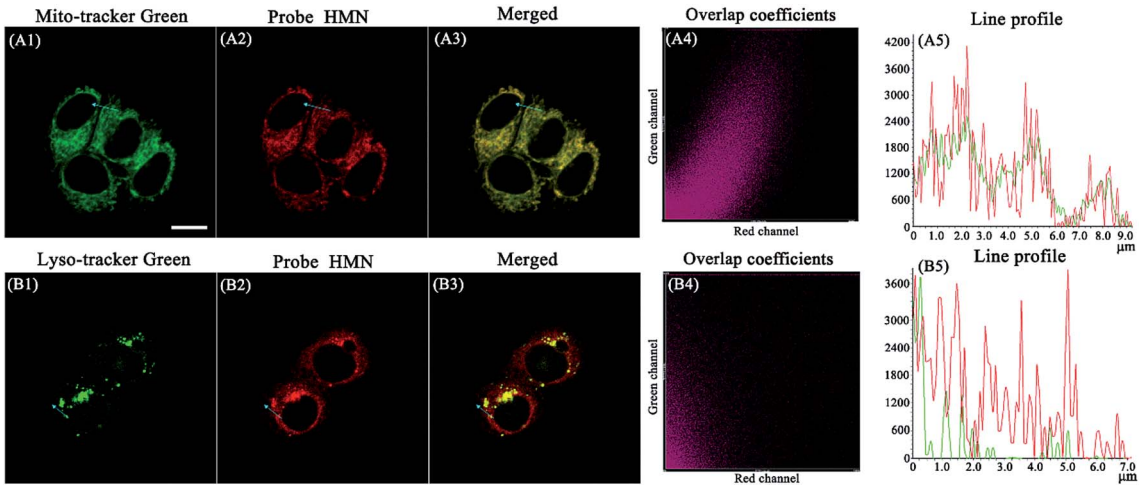

Fig. 8 The images of living HeLa cells pre-treated with **HMN** (5 μM) for 30 min and subsequently co-incubated with (A) Mito-Tracker Green (1 μM) or (B) Lyso-Tracker Green (1 μM) for 10 min. (A1, B1) Green channel images of Mito-Tracker Green and Lyso-Tracker Green (λ_{ex} = 488 nm, λ_{em} = 500–535 nm); (A2, B2) red channel images of probe **HMN** (λ_{ex} = 561 nm, λ_{em} = 595–630 nm); (A3, B3) merged green and red channel images; (A4, B4) the overlap coefficients of green and red channel images; (A5, B5) the intensity profile of the ROI in merged images. Scale bar: 10 μm.

concentration levels)) in three-channel fluorescence imaging, which is in accordance with the spectral performances in aqueous solution. Thus, **HMN** not only can simultaneously distinguish three groups of biothiols (Cys/Hcy, GSH, and H_2S (at relatively high concentration levels)) in aqueous and biological systems *via* three-channel fluorophotometric assay, but is also appropriate for imaging applications able to simultaneously distinguish Cys/Hcy and endogenous H_2S (at relatively low concentration levels) using the green and blue channels.

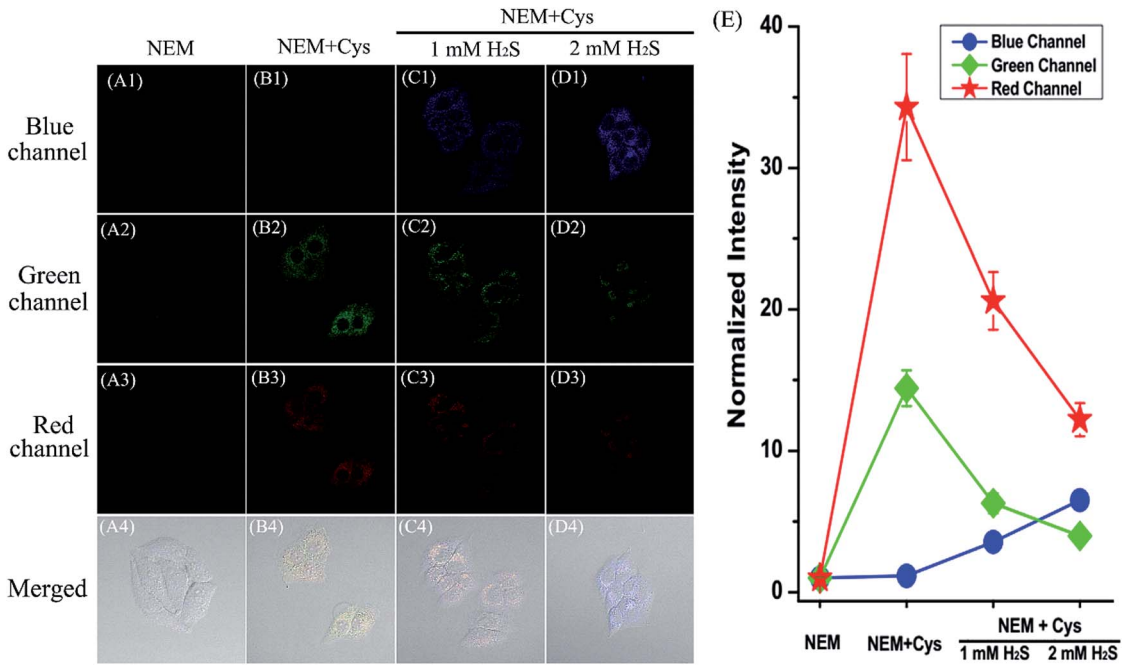

Fig. 9 Fluorescence images of probe **HMN** sequentially sensing Cys and H_2S in living HeLa cells using confocal fluorescence imaging. (A) Cells were pre-treated with NEM (0.5 mM, 30 min), subsequently incubated with probe **HMN** (5 μM, 30 min), and then imaged; (B) cells were pre-treated with NEM (0.5 mM, 30 min), subsequently incubated with Cys (250 μM, 15 min) and probe **HMN** (5 μM, 30 min), and then imaged; (C and D) cells were pre-treated with NEM (0.5 mM, 30 min), subsequently incubated with Cys (250 μM, 15 min) and probe **HMN** (5 μM, 30 min), and continued to be treated with 1 or 2 mM Na_2S for 25 min, and then imaged. The fluorescence images were captured from the blue channel of 465–500 nm (first row), green channel of 525–555 nm (second row), and red channel of 595–630 nm with excitation (third row) at 405, 488, and 561 nm, respectively. Fourth row: merged bright field images with blue, green, and red channel images. Scale bar: 20 μm. (E) The normalized average fluorescence intensity of the blue, green, and red channel in (A–D). The normalized intensity of group (A) in the respective channels is taken as the reference standard. Data are expressed as the mean ± SD of three parallel experiments.

To confirm the distribution of **HMN** at subcellular levels, co-localization experiments were carried out in HeLa cells. The cells were pre-treated with **HMN** (5 μM) for 25 min and Mito-Tracker Green or Lyso-Tracker Green (1 μM) was subsequently added and incubated for another 5 min. As shown in Fig. 8A, as expected, the fluorescence image of **HMN** in the red channel almost completely overlaps with that of the mitochondrial probe (Mito-Tracker Green) in the green channel, with a high overlap coefficient (0.869). In contrast, the fluorescence image of **HMN** has an extremely inefficient overlap with that of the lysosomal probe (Lyso-Tracker Green) and the overlap coefficient is as low as 0.476 (Fig. 8B). It might be that the electropositive **HMN** tends to localize to the cellular mitochondria with a negative potential.[22,47] Thus, probe **HMN** is a potentially excellent tool for studying mitochondrial biothiols.

Sequential sensing of biothiols in living cells

After reaching the goal of simultaneous discrimination of biothiols, we further employed **HMN** to sequentially sense biothiols in living cells. The cells were firstly treated with NEM to scavenge the inherent thiols, followed by the addition of Cys (250 μM) and incubation for 20 min. Cells were subsequently incubated for another 30 min with **HMN** (5 μM). The bright emission induced by Cys is observed in both the green and red channels (Fig. 9A and B). However, with increasing dosages of Na_2S (1–2 mM), the emission is gradually weakened in the green and red channels, and at the same time a significant enhancement of fluorescence appears in the blue channel (Fig. 9C and D). This could be interpreted to mean that the encounter of **HMN** with cellular Cys produces the red fluorescent compound **HBTMC1** and a green fluorescent NBD derivative **NBD-Cys**, which further reacts with H_2S to yield a fluorescent compound **HBTMC1-SH** with blue emission and a non-fluorescent compound **NBD-SH**, respectively. Similarly, the red emission generated by the reaction of **HMN** with cellular GSH is quenched by the subsequently added H_2S, and a gradual increase of blue fluorescence arises simultaneously (Fig. S15†). These results indicated that probe **HMN** is capable of sequentially sensing biothiols in biological contexts using three-color fluorescence imaging, in addition to simultaneous discrimination of biothiols from each other.

Conclusions

In summary, by hybridizing a hydroxyphenyl benzothiazole merocyanine (HBTMC) dye and a nitro benzoxadiazole (NBD) chromophore, we have developed a single fluorescent probe, **HMN**, for simultaneously distinguishing Cys/Hcy, GSH, and H_2S from each other and sequentially sensing Cys/Hcy/GSH and H_2S *via* a multi-channel fluorometric method for the first time. When responding to respective biothiols, **HMN** exhibits multiple sets of fluorescence signals in three distinct emission bands (blue-green-red), which possess 61 and 63 nm interval distances between two adjacent bands, respectively. The probe can also sense H_2S at different concentration levels with changes of fluorescence in the blue and red emission bands. The excellent performance of **HMN** in the three-channel fluorescence imaging indicates that the probe can be applied to simultaneously discriminate biothiols from each other and sequentially sense Cys/Hc/GSH and H_2S in biological contexts. The development of this unique probe may open an avenue to design fluorescent probes for the discrimination and sequential detection of biothiols, and provides a promising tool for unveiling the interrelated roles of biothiols in various physiological and pathological conditions.

Acknowledgements

This work was financially supported by NSFC (21472067, 21672083, and 21605059), SDNSF (ZR2016BB26), Taishan Scholar Foundation (TS 201511041), and the start-up fund of the University of Jinan (309-10004 and 160100136).

Notes and references

1 G. I. Giles, K. M. Tasker and C. Jacob, *Free Radical Biol. Med.*, 2001, **31**, 1279.
2 Z. A. Wood, E. Schröder, J. R. Harris and L. B. Poole, *Trends Biochem. Sci.*, 2003, **28**, 32.
3 G. I. Giles and C. Jaco, *Biol. Chem.*, 2005, **383**, 375.
4 M. Kemp, Y.-M. Go and D. P. Jones, *Free Radical Biol. Med.*, 2008, **44**, 921.
5 M. T. V. ishanina, M. Libiad and R. Banerjee, *Nat. Chem. Biol.*, 2015, **11**, 457.
6 L. Li, P. Rose and P. K. Moore, *Annu. Rev. Pharmacol.*, 2011, **51**, 169.
7 G. Yang, L. Wu, B. Jiang, B. Yang, J. Qi, K. Cao, Q. Meng, A. K. Mustafa, W. Mu, S. Zhang, S. H. Snyder and R. Wang, *Science*, 2008, **322**, 587.
8 O. Kabil and R. Banerjee, *J. Biol. Chem.*, 2010, **285**, 21903.
9 N. C. Sturgess, R. Z. Kozlowski, C. A. Carrington, C. N. Hales and J. M. L. Ashford, *Br. J. Pharmacol.*, 1988, **95**, 83.
10 G. Yang, L. Wu and R. Wang, *FASEB J.*, 2006, **20**, 553.
11 S. Singh, D. Padovani, R. A. Leslie, T. Chiku and R. Banerjee, *J. Biol. Chem.*, 2009, **284**, 22457.
12 J. E. Dominy and M. H. Stipanuk, *Nutr. Rev.*, 2004, **62**, 348.
13 S. Y. Zhang, C.-N. Ong and H.-M. Shen, *Cancer Lett.*, 2004, **208**, 143.
14 M. E. Anderson, *Chem.-Biol. Interact.*, 1998, **111**, 1.
15 T. D. Dalton, H. G. Shertzer and A. Puga, *Annu. Rev. Pharmacol. Toxicol.*, 1999, **39**, 67.
16 P. N. Prasad, Bioimaging: Principles and Techniques, in *Introduction to Biophotonics*, John Wiley & Sons, Inc., 2003, ch. 7.
17 J. Chan, S. C. Dodani and C. J. Chang, *Nat. Chem.*, 2012, **4**, 973.
18 X. Chen, T. Pradhan, F. Wang, J. S. Kim and J. Yoon, *Chem. Rev.*, 2012, **112**, 1910.
19 A. Chattopadhyay, S. Shrivastava and A. Chaudhuri, Membrane Fluorescent Probes: Insights and Perspectives, in *Fluorescent Analogues of Biomolecular Building Blocks: Design and Applications*, John Wiley & Sons, Inc., 2016, ch. 15.

20 K. P. Carter, A. M. Young and A. E. Palmer, *Chem. Rev.*, 2014, **114**, 4564.
21 A. P. Demchenko, *Introduction to fluorescence sensing*, Springer, 2015.
22 H. Zhu, J. Fan, J. Du and X. Peng, *Acc. Chem. Res.*, 2016, **49**, 2115.
23 L. A. Montoya and M. D. Pluth, *Anal. Chem.*, 2014, **86**, 6032.
24 Y. Chen, C. Zhu, Z. Yang, J. Chen, Y. He, Y. Jiao, W. He, L. Qiu, J. Cen and Z. Guo, *Angew. Chem., Int. Ed.*, 2013, **52**, 1688.
25 S. Paul, S. Goswami and C. D. Mukhopadhyay, *New J. Chem.*, 2015, **39**, 8940.
26 X. Feng, T. Zhang, J.-T. Liu, J.-Y. Miao and B.-X. Zhao, *Chem. Commun.*, 2016, **52**, 3131.
27 H. S. Jung, X. Chen, J. S. Kim and J. Yoon, *Chem. Soc. Rev.*, 2013, **42**, 6019.
28 L.-Y. Niu, Y.-Z. Chen, H.-R. Zheng, L.-Z. Wu, C.-H. Tung and Q.-Z. Yang, *Chem. Soc. Rev.*, 2015, **44**, 6143.
29 V. S. Lin, W. Chen, M. Xian and C. J. Chang, *Chem. Soc. Rev.*, 2015, **44**, 4596.
30 J. Liu, Y.-Q. Sun, Y. Huo, H. Zhang, L. Wang, P. Zhang, D. Song, Y. Shi and W. Guo, *J. Am. Chem. Soc.*, 2014, **136**, 574.
31 H. Zhang, R. Liu, J. Liu, L. Li, P. Wang, S. Q. Yao, Z. Xu and H. Sun, *Chem. Sci.*, 2016, **7**, 256.
32 W. Chen, H. Luo, X. Liu, J. W. Foley and X. Song, *Anal. Chem.*, 2016, **88**, 3638.
33 Q. Hu, C. Yu, X. Xia, F. Zeng and S. Wu, *Biosens. Bioelectron.*, 2016, **81**, 341.
34 H. Li, W. Peng, W. Feng, Y. Wang, G. Chen, S. Wang, S. Li, H. Li, K. Wang and J. Zhang, *Chem. Commun.*, 2016, **52**, 4628.
35 Z.-H. Fu, X. Han, Y. Shao, J. Fang, Z.-H. Zhang, Y.-W. Wang and Y. Peng, *Anal. Chem.*, 2017, **89**, 1937.
36 L.-Y. Niu, H.-R. Zheng, Y.-Z. Chen, L.-Z. Wu, C.-H. Tunga and Q.-Z. Yang, *Analyst*, 2014, **139**, 1389.
37 M. D. Hammers and M. D. Pluth, *Anal. Chem.*, 2014, **86**, 7135.
38 X. Gao, X. Li, L. Li, J. Zhou and H. Ma, *Chem. Commun.*, 2015, **51**, 9388.
39 M. Ren, B. Deng, X. Kong, K. Zhou, K. Liu, G. Xu and W. Lin, *Chem. Commun.*, 2016, **52**, 6415.
40 K. Schöller, S. Küpfer, L. Baumann, P. M. Hoyer, D. de Courten, R. M. Rossi, A. Vetushka, M. Wolf, N. Bruns and L. J. Scherer, *Adv. Funct. Mater.*, 2014, **24**, 5194.
41 D. Oushiki, H. Kojima, T. Terai, M. Arita, K. Hanaoka, Y. Urano and T. Nagano, *J. Am. Chem. Soc.*, 2010, **132**, 2795.
42 P. Xu, T. Gao, M. Liu, H. Zhang and W. Zeng, *Analyst*, 2015, **140**, 1814.
43 S. F. Betz, *Protein Sci.*, 1993, **2**, 1551.
44 P. J. Hogg, *Trends Biochem. Sci.*, 2003, **28**, 210.
45 G. Yang, L. Wu, B. Jiang, W. Yang, J. Qi, K. Cao, Q. Meng, A. K. Mustafa, W. Mu, S. Zhang, S. H. Snyder and R. Wang, *Science*, 2008, **322**, 587.
46 Y. Qian, J. Karpus, O. Kabil, S.-Y. Zhang, H.-L. Zhu, R. Banerjee, J. Zhao and C. He, *Nat. Commun.*, 2011, **2**, 1506.
47 B. Kadenbach, *Biochim. Biophys. Acta, Bioenerg.*, 2003, **1604**, 77.